An analytic model of plasma-neutral coupling in the heliosphere plasma

D A S T G E E R   S H A I K H[1,2] and B.   D A S G U P T A[2]

[1]Department of Physics, University of Alabama at Huntsville, Huntsville, AL 35805, USA
(dastgeer.shaikh@uah.edu)

[2]Center for Space Physics and Aeronomic Research (CSPAR),
University of Alabama at Huntsville, Huntsville, AL 35805, USA

Abstract. We have developed an analytic model to describe coupling of plasma and neutral fluids in the partially ionized heliosphere plasma medium. The sources employed in our analytic model are based on a κ-distribution as opposed to the Maxwellian distribution function. Our model uses the κ-distribution to analytically model the energetic neutral atoms that result in the heliosphere partially ionized plasma from charge exchange with the protons and subsequently produce a long tail, which is otherwise not describable by the Maxwellian distribution. We present our analytic formulation and describe major differences in the sources emerging from these two distinct distributions.

1. Introduction

With the Voyager spacecraft now in the heliosheath (see Fig. 1), the *in situ* character of the solar wind plasma can be explored. Surprisingly, the supersonic solar wind plasma, probed by the ACE/WIND/Cluster spacecrafts near 1 astronomical unit (AU), depicts an entirely different character when contrasted with the Voyager I and 2 observations in the heliosheath region (typically beyond 84 AU) (Goldstein et al. 1995; Zank 1999; Stone et al. 2005; Burlaga et al. 2005, 2006, 2008; Decker et al. 2005; Richardson et al. 2008; Burlaga and Ness 2009). Figure 1 shows an idealized cartoon reflecting our current understanding based on theory, simulations and modeling together with observations. Little is known about the physical processes that govern the intricate multiscale (associated with waves, structures and turbulence) interactions outlined in Fig. 1. The supersonic solar wind (SW) plasma interacts with local interstellar medium (LISM) neutral hydrogen (H) gas through charge exchange leading to the creation of energetic pick-up ions (PUI). The SW is decelerated, compressed and heated at a shock, the termination shock (TS), across which it develops small scale turbulence (Shukla 1978; Shaikh et al. 2006; Heerikhuisen et al. 2007; Mendonca and Shukla 2007; Shaikh and Zank 2008, 2010; Shaikh in press). In the heliosheath region, the nonlinear structures, such as magnetic hole and humps are found (Burlaga et al. 2008, 2009). The SW protons continue to interact with neutrals via charge exchange to produce significant number of pick-up ions. Both in the supersonic and subsonic SW (at least in the outer heliosphere), the pressure associated with the PUIs exceeds that of the solar wind protons (Burlaga et al. 2009).

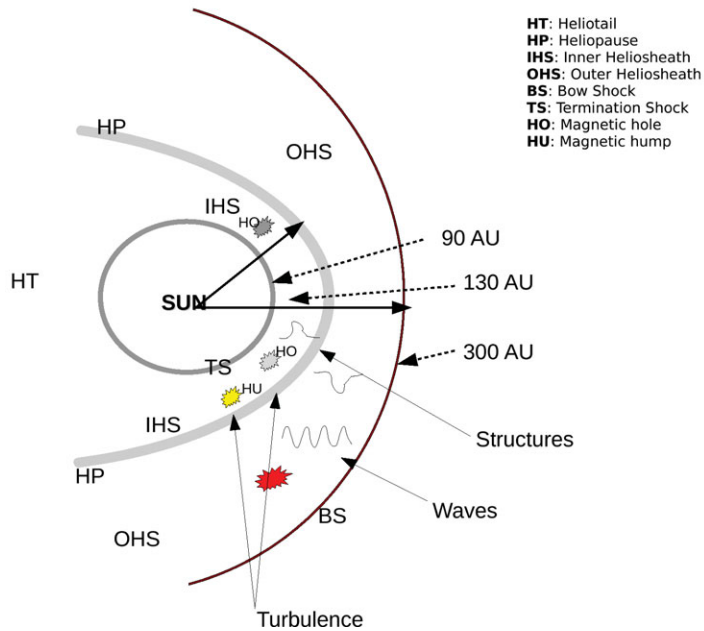**Heliosphere: region filled with solar wind plasma and bounded by HP**

Figure 1. (Colour online) Schematic overview of different regions in the global heliosphere. The solar wind emanating from the Sun propagates outward and interacts with partially ionized interstellar gas predominantly via charge exchange, and creates pick up ions (PUIs). At the termination shock (TS), the supersonic solar wind (SW) decelerated, heated and compressed becoming subsonic, in the heliosheath, and again interacts with interstellar neutrals via charge exchange before it reaches heliopause (HP). The subsonic SW flows down into the heliotail. Magnetic structures, such as magnetic holes/humps, are observed in heliosheath plasma. During its journey from the Sun to the HP, the SW plasma develops multitude of length and time-scales that interact with the partially ionized interstellar gas, TS, and nonlinear structures develop in a complex manner.

Both Voyager 1 and Voyager 2 are reporting a number of puzzling observations that were not anticipated by the existing analytic or simulation models. An intriguing example is that of magnetic field distribution. The latter is lognormal in supersonic SW, whereas it exhibits a Gaussian distribution in subsonic heliosheath. Surprisingly, Voyager 2 indicates that the magnetic field distribution is lognormal in the subsonic heliosheath plasma. The source of this apparent discrepancy in the magnetic field distributions reported by Voyager 1 & Voyager 2 in the heliosheath is not known. Another example is that of plasma in heliosheath which is compressed, turbulent and is an admixture of waves, fluctuations and magnetic structures (magnetic hole/hump, see Sec. 2 for details) (Burlaga 2006, 2009). The effect of PUIs on the formation and evolution of nonlinear magnetic structures, waves and fluctuations in outer heliosphere and the heliosheath plasma are an open question. These issues continue to pose severe challenges to our understanding of the heliosheath plasma.

Although there exists wealth of *in situ* measurements by the Voyager spacecrafts, they do not provide much information about the global structure of the heliosphere interactions. For instance, the coupling of plasma protons with the interstellar

neutral atoms has traditionally been done through Maxwellian sources. However, careful studies have revealed that the distribution of hydrogen neutral (after charge exchanging, they turn into energetic neutral atoms, ENA) does not exactly follow a Maxwellian functions. Recently, Prested et al. (2008) used a κ-distribution for the ENA parent population to obtain ENA maps. The advantage of using this distribution, as opposed to a Maxwellian, is that it has a power-law tail, and is therefore capable of producing ENAs at suprathermal energies. Now there has been an increasing consensus that the plasma and neutral fluids follow nearly κ-distribution (Heerikhuisen et al. 2008).

A realistic modeling of the heliosheath plasma, one that includes a self-consistent treatment of the PUIs, is therefore critically important and essential to our understanding of the highly variable heliosphere plasma. The central theme of this paper is therefore to model complex coupling between plasma and neutral fluids via κ-distribution as opposed to the Maxwellian distribution. Note here that the κ-distribution modifies the charge-exchange interactions in fluid equations. The κ-distribution emphasizes charge exchange by high-temperature protons. We will investigate the effects of the κ-distribution in heliosphere plasma turbulence for single fluid plasma-neutral coupled turbulence models.

In Sec. 2, we describe κ-distribution for neutral and plasma distributions and derive sources for the complex coupling interactions between the two distinct fluids. Section 3 describes complete source terms for the coupling interactions. Finally, a summary is presented in Sec. 5.

2. Plasma neutral coupling via κ-distribution source

The charge-exchange terms can be obtained from the Boltzmann transport equation that describes the evolution of a neutral distribution function $f(\mathbf{r}, \mathbf{v}, t)$ in a six-dimensional phase space defined respectively by position and velocity vectors (x, v_x, v_y, v_z) at each time t. Here we follow Pauls et al. (1995) in computing the charge-exchange terms, based on κ-distribution functions, from various moments of the Boltzmann equation. The Boltzmann equation for the neutral distribution contains a source term proportional to the proton distribution function f_p and a loss term proportional to the neutral distribution function f_n.

$$\frac{\partial}{\partial t} f_p(\mathbf{r}, \mathbf{v}, t) + \mathbf{v} \cdot \nabla f_p(\mathbf{r}, \mathbf{v}, t) + \frac{\mathbf{F}}{m} \cdot \nabla_v f_p(\mathbf{r}, \mathbf{v}, t)$$

$$= f_n(\mathbf{r}, \mathbf{v}, t) \int f_p(\mathbf{r}, \mathbf{v_p}, t) |\mathbf{v_p} - \mathbf{v}| \, \sigma_{ex}(v_{rel}) d^3 \mathbf{v_p}$$

$$- f_p(\mathbf{r}, \mathbf{v}, t) \int f_n(\mathbf{r}, \mathbf{v_n}, t) |\mathbf{v_n} - \mathbf{v}| \, \sigma_{ex}(v_{rel}) d^3 \mathbf{v_n}, \qquad (2.1)$$

where, $\sigma_{ex}(v_{rel})$ is the charge-exchange cross-section. The charge-exchange parameter has a logarithmically weak dependence on the relative speed ($v_{rel} = |u_p - v_n|$) of the neutrals and the protons through $\sigma_{ex} = [(2.1 - 0.092 \ln(v_{rel}))10^{-7} \text{ cm}]^2$ (Fite et al. 1962). This cross-section is valid as long as energy does not exceed 1 eV, which usually is the case in the inner/outer heliosphere. Beyond 1 eV energy, this cross-section yields a higher neutral density. This issue is not applicable to our model and, hence, we will not consider it here. The density, momentum and energy of

the thermally equilibrated Maxwellian proton and neutral fluids can be computed from (2.1) by using the zeroth, first and second moments $\int f_\xi d^3\xi$, $\int m\xi f_\xi d^3\xi$ and $\int m\xi^2/2 f_\xi d^3\xi$ respectively, where $\xi = u_p$ or v_n. As charge exchange conserves the density of the proton and neutral fluids, there are no sources in the corresponding continuity equations. We, therefore, need not compute the zeroth moment of the distribution function. Computing directly the first moment from (2.1), we obtain the neutral fluid momentum equation.

A similar evolution equation can be written for the neutral distribution function $f_n(\mathbf{r}, \mathbf{v_n}, t)$. We consider the case where both $f_p(\mathbf{r}, \mathbf{v_p}, t)$ and $f_n(\mathbf{r}, \mathbf{v_n}, t)$ are given by a κ-distribution of the following type:

$$f_p(\mathbf{r}, \mathbf{v_p}) = \frac{n_p}{\pi^{\frac{3}{2}} v_{T_p}^3} \frac{\Gamma(\kappa+1)}{\kappa^{\frac{3}{2}} \Gamma\left(\kappa-\frac{1}{2}\right)} \left[1 + \frac{(\mathbf{v_p} - \mathbf{U_p})^2}{\kappa v_{T_p}^2}\right]^{-(\kappa+1)}, \quad (2.2)$$

$$f_n(\mathbf{r}, \mathbf{v_n}) = \frac{n_n}{\pi^{\frac{3}{2}} v_{T_n}^3} \frac{\Gamma(\kappa+1)}{\kappa^{\frac{3}{2}} \Gamma\left(\kappa-\frac{1}{2}\right)} \left[1 + \frac{(\mathbf{v_n} - \mathbf{U_n})^2}{\kappa v_{T_n}^2}\right]^{-(\kappa+1)}. \quad (2.3)$$

We first evaluate the following integral:

$$\beta_p(\mathbf{r}, \mathbf{v}, t) = \sigma_{ex}(v_{rel}) \int f_p(\mathbf{r}, \mathbf{v_p}, t) \left|\mathbf{v_p} - \mathbf{v}\right| d^3\mathbf{v_p}, \quad (2.4)$$

where $\sigma_{ex}(v_{rel})$ is taken out of the integral, as it varies slowly with respect to (v_{rel}). The integral (2.4) is fully written as

$$\beta_p(\mathbf{r}, \mathbf{v}, t) = \sigma_{ex}(v_{rel}) \frac{n_p}{\pi^{\frac{3}{2}} v_{T_p}^3} A_\kappa \int \left[1 + \frac{(\mathbf{v_p} - \mathbf{U_p})^2}{\kappa v_{T_p}^2}\right]^{-(\kappa+1)} \left|\mathbf{v_p} - \mathbf{v}\right| d^3\mathbf{v_p}, \quad (2.5)$$

with

$$A_\kappa = \frac{\Gamma(\kappa+1)}{\kappa^{\frac{3}{2}} \Gamma\left(\kappa-\frac{1}{2}\right)}.$$

We write,

$$\mathbf{v_p} - \mathbf{U_p} = (\mathbf{v_p} - \mathbf{v}) - (\mathbf{U_p} - \mathbf{v})$$

and define new variables as

$$\mathbf{V} = (\mathbf{v_p} - \mathbf{v})/\sqrt{\kappa v_{T_p}^2}, \quad \mathbf{x} = (\mathbf{U_p} - \mathbf{v})/\sqrt{\kappa v_{T_p}^2};$$

with the new variables, the integral in (2.5) becomes,

$$\beta_p(\mathbf{r}, \mathbf{v}, t) = \sigma_{ex}(v_{rel}) \frac{n_p}{\pi^{\frac{3}{2}} v_{T_p}^3} \left(\kappa v_{T_p}^2\right)^{3/2} \sqrt{\kappa v_{T_p}^2} A_\kappa \int_{-\infty}^{\infty} \left[1 + (\mathbf{V} - \mathbf{x})^2\right]^{-(\kappa+1)} V d^3\mathbf{V}, \quad (2.6)$$

where we have used,

$$\left|\mathbf{v_p} - \mathbf{v}\right| = \sqrt{\kappa v_{T_p}^2} V; \quad d^3\mathbf{v_p} = \left(\kappa v_{T_p}^2\right)^{3/2} d^3\mathbf{V},$$

and the constant before the integral in (2.6) is,

$$\sigma_{ex}(v_{rel}) \frac{n_p}{\pi^{\frac{3}{2}} v_{T_p}^3} \left(\kappa v_{T_p}^2\right)^{3/2} \sqrt{\kappa v_{T_p}^2} \frac{\Gamma(\kappa+1)}{\kappa^{\frac{3}{2}} \Gamma\left(\kappa-\frac{1}{2}\right)} = \sigma_{ex} \frac{n_p v_{T_p}}{\pi^{\frac{3}{2}}} \frac{\sqrt{\kappa} \, \Gamma(\kappa+1)}{\Gamma\left(\kappa-\frac{1}{2}\right)}.$$

We now proceed to evaluate the integral (2.6). In spherical coordinate,

$$d^3\mathbf{V} = V^2 dv \sin\theta \, d\theta \, d\phi,$$

where θ is the angle between $\mathbf{V}$ and $\mathbf{x}$, after performing the ϕ integration with $\mu = \cos\theta$,

$$I = 2\pi \int_0^\infty V^3 dV \int_{-1}^1 d\mu (1 + V^2 - 2Vx\mu + x^2)^{-(\kappa+1)}. \tag{2.7}$$

This integration becomes,

$$I = 2\left[\int_0^x z^2(1+z^2)^{-\kappa}dz + x^2\int_0^x (1+z^2)^{-\kappa}dz + 2x\int_x^\infty z(1+z^2)^{-\kappa}dz\right],$$

with $\mathbf{x} = (\mathbf{U_p} - \mathbf{v})/\sqrt{\kappa v_{T_p}^2}$. We now proceed to determine the explicit values of the above definite integrals. The first two integrals are given in terms of the hypergeometric functions, $_2F_1$, which are

$$\int_0^x z^2(1+z^2)^{-\kappa}dz = \frac{x^3}{3} \, _2F_1\left(\frac{3}{2}, \kappa; \frac{5}{2}; -x^2\right),$$

$$x^2\int_0^x (1+z^2)^{-\kappa}dz = x \, _2F_1\left(\frac{1}{2}, \kappa; \frac{3}{2}; -x^2\right),$$

where the Hypergeometric function $_2F_1(a, b, c, z)$ (with a, b, c are constant numbers and z is the variable) is expressed as a power series in z:

$$_2F_1(a, b; c; z) = 1 + \frac{ab}{c}\frac{z}{1!} + \frac{a(a+1)b(b+1)}{c(c+1)}\frac{z^2}{2!}$$

$$+ \frac{a(a+1)(a+2)b(b+1)(b+2)}{c(c+1)(c+2)}\frac{z^3}{3!} + \cdots \tag{2.8}$$

Using Kummer identity for hypergeometric functions,

$$_2F_1(a, b; c; z) = \, _2F_1(b, a; c; z) = (1-z)^{-b}{}_2F_1[b, c-a; c; z/(z-1)], \tag{2.8a}$$

$$_2F_1\left(\frac{3}{2}, \kappa; \frac{5}{2}; -x^2\right) = (1+x^2)^{-\kappa}{}_2F_1\left(\frac{5-3}{2}, \kappa; \frac{5}{2}; \frac{x^2}{1+x^2}\right)$$

$$= (1+x^2)^{-\kappa}{}_2F_1\left(1, \kappa; \frac{5}{2}; \frac{x^2}{1+x^2}\right). \tag{2.8b}$$

Similarly,

$$_2F_1\left(\frac{1}{2}, \kappa; \frac{3}{2}; -x^2\right) = (1+x^2)^{-\kappa}{}_2F_1\left(1, \kappa; \frac{3}{2}; \frac{x^2}{1+x^2}\right). \tag{2.8c}$$

The last integral can be evaluated easily

$$\int_x^\infty z(1+z^2)^{-\kappa}dz = \left.\frac{(1+z^2)^{-\kappa+1}}{2(-\kappa+1)}\right|_x^\infty = \frac{(1+x^2)^{-\kappa+1}}{2(\kappa-1)} \quad (\kappa \text{ must be} > 1).$$

Collecting the above terms, the integral $\beta_p(\mathbf{r}, \mathbf{v})$ is,

$$\beta_p(\mathbf{r}, \mathbf{v}, t) = \frac{2n_p \sigma_{ex} v_{T_p}}{\sqrt{\pi \kappa}} \frac{1}{x} \frac{\Gamma(\kappa+1)}{\Gamma\left(\kappa - \frac{1}{2}\right)} (1+x^2)^{-\kappa} \left[x^2 \, {}_2F_1\left(1, \kappa; \frac{3}{2}; \frac{x^2}{1+x^2}\right) \right.$$

$$\left. + \frac{x^2}{3} \, {}_2F_1\left(1, \kappa; \frac{5}{2}; \frac{x^2}{1+x^2}\right) + \frac{1+x^2}{\kappa-1} \right]; \quad x = |\mathbf{U_p} - \mathbf{v}| / \sqrt{\kappa v_{T_p}^2}. \quad (2.9)$$

An approximate value of the above expression in the two limits $\sqrt{\kappa}\, x \ll 1$ and $x \gg 1$ can be obtained as follows:

$$\sqrt{\kappa}\, x \ll 1: \qquad \beta = \frac{2n_p \sigma_{ex} v_{T_p}}{\sqrt{\pi \kappa}} \frac{\Gamma(\kappa+1)}{\Gamma\left(\kappa-\frac{1}{2}\right)} \left[\frac{1}{\kappa-1} + \frac{(\mathbf{U_p} - \mathbf{v})^2}{3\kappa v_{T_p}^2} \right]. \qquad (2.10)$$

$$x \gg 1: \qquad \beta = n_p \sigma_{ex} \sqrt{\frac{4 v_{T_p} \Gamma^2(\kappa+1)}{\pi \kappa(\kappa-1)\Gamma^2\left(\kappa-\frac{1}{2}\right)} + (\mathbf{U_p} - \mathbf{v})^2}. \qquad (2.11)$$

Note that in an asymptotic limit, the Gamma functions for large argument is

$$\lim_{\kappa \to \infty} \kappa^{b-a} \frac{\Gamma(\kappa+a)}{\Gamma(\kappa+b)} \to 1, \quad \Rightarrow \quad \lim_{\kappa \to \infty} \Gamma(\kappa+a) \simeq \kappa^a \Gamma(\kappa).$$

3. Complete expressions for the source terms

To find the source terms, we take the moments of (2.1) by multipling both sides with various powers of the velocity $\mathbf{v}$. The zeroth-order moment would contribute to the source term of the mass continuity equation, the first-order moment would contribute to the source term of the momentum equation and the second-order moment would contribute to the source term of the energy equation. The moments for the left-hand terms in (2.1) are well-known, so we shall show the moments of the right-hand terms, using κ-distribution for f_p and f_n. We derive full expression for the integrals on the right-hand side of (2.1) by using the complete expression for the integral for $\beta_p(\mathbf{r}, \mathbf{v}, t)$ given by (2.9) without any approximation.

As the charge-exchange process conserves the proton and neutral densities, there will be no source term for the mass continuity term, so we need not calculate the zeroth moment. Hence we start with the first moment of the right-hand side of (2.1). With

$$f_n(\mathbf{r}, \mathbf{v}) = \frac{n_n}{\pi^{\frac{3}{2}} v_{T_n}^3} \frac{\Gamma(\kappa+1)}{\kappa^{\frac{3}{2}} \Gamma\left(\kappa-\frac{1}{2}\right)} \left[1 + \frac{(\mathbf{v}-\mathbf{U_n})^2}{\kappa v_{T_n}^2} \right]^{-(\kappa+1)} = f_n(\mathbf{r}, \mathbf{v} - \mathbf{U_n}),$$

$$\text{and} \qquad \beta_p(\mathbf{r}, \mathbf{v}, t) \equiv \beta_p(\mathbf{r}, x, t) = \beta_p(\mathbf{r}, \mathbf{U_p} - \mathbf{v}).$$

The production term for momentum transport is

$$Q_{MP} = \int_0^\infty d^3 v\, \mathbf{v} f_n(\mathbf{r}, \mathbf{v} - \mathbf{U_n}) \beta_p(\mathbf{r}, \mathbf{U_p} - \mathbf{v}),$$

$$= \int_0^\infty d^3 v\, \mathbf{U_n} f_n(\mathbf{r}, \mathbf{v} - \mathbf{U_n}) \beta_p[\mathbf{r}, (\mathbf{U_p} - \mathbf{U_n}) - (\mathbf{v} - \mathbf{U_n})]$$

$$+ \int_0^\infty d^3v (\mathbf{v} - \mathbf{U_n}) f_n(\mathbf{r}, \mathbf{v} - \mathbf{U_n}) \beta_p[\mathbf{r}, (\mathbf{U_p} - \mathbf{U_n}) - (\mathbf{v} - \mathbf{U_n})],$$

$$= \mathbf{U_n} \int_0^\infty d^3u f_n(\mathbf{r}, \mathbf{u}) \beta_p[\mathbf{r}, (\Delta\mathbf{U} - \mathbf{u})] + \int_0^\infty d^3u \mathbf{u} f_n(\mathbf{r}, \mathbf{u}) \beta_p[\mathbf{r}, (\Delta\mathbf{U} - \mathbf{u})], \quad (3.1)$$

where we used, $\mathbf{u} = \mathbf{v} - \mathbf{U_n}, \quad \Delta\mathbf{U} = \mathbf{U_p} - \mathbf{U_n}$.

The production term for energy transport is

$$Q_{EP} = \int_0^\infty d^3v |\mathbf{v}|^2 f_n(\mathbf{r}, \mathbf{v} - \mathbf{U_n}) \beta_p(\mathbf{r}, \mathbf{U_p} - \mathbf{v}),$$

$$= \int_0^\infty d^3v |\mathbf{v} - \mathbf{U_n}|^2 f_n(\mathbf{r}, \mathbf{v} - \mathbf{U_n}) \beta_p(\mathbf{r}, \mathbf{U_p} - \mathbf{v})$$

$$+ 2\mathbf{U_n} \cdot \int_0^\infty d^3v \mathbf{v} f_n(\mathbf{r}, \mathbf{v} - \mathbf{U_n}) \beta_p(\mathbf{r}, \mathbf{U_p} - \mathbf{v})$$

$$- U_n^2 \int_0^\infty d^3v f_n(\mathbf{r}, \mathbf{v} - \mathbf{U_n}) \beta_p(\mathbf{r}, \mathbf{U_p} - \mathbf{v}),$$

$$= \int_0^\infty d^3v |\mathbf{v} - \mathbf{U_n}|^2 f_n(\mathbf{r}, \mathbf{v} - \mathbf{U_n}) \beta_p(\mathbf{r}, \mathbf{U_p} - \mathbf{v})$$

$$+ 2\mathbf{U_n} \cdot \int_0^\infty d^3v (\mathbf{v} - \mathbf{U_n}) f_n(\mathbf{r}, \mathbf{v} - \mathbf{U_n}) \beta_p(\mathbf{r}, \mathbf{U_p} - \mathbf{v})$$

$$+ 2U_n^2 \int_0^\infty d^3v f_n(\mathbf{r}, \mathbf{v} - \mathbf{U_n}) \beta_p(\mathbf{r}, \mathbf{U_p} - \mathbf{v})$$

$$- U_n^2 \int_0^\infty d^3v f_n(\mathbf{r}, \mathbf{v} - \mathbf{U_n}) \beta_p(\mathbf{r}, \mathbf{U_p} - \mathbf{v}). \quad (3.2)$$

As before, we introduce the variables $\mathbf{u} = \mathbf{v} - \mathbf{U_n}; \quad \Delta\mathbf{U} = \mathbf{U_p} - \mathbf{U_n}$ and write $\beta_p(\mathbf{r}, \mathbf{U_p} - \mathbf{v}) = \beta_p(\mathbf{r}, (\mathbf{U_p} - \mathbf{U_n}) - (\mathbf{v} - \mathbf{U_n})) = \beta_p(\mathbf{r}, \Delta\mathbf{U} - \mathbf{u})$. Expression (3.2) can be written as

$$Q_{EP} = \int_0^\infty d^3u u^2 f_n(\mathbf{r}, \mathbf{u}) \beta_p(\mathbf{r}, \Delta\mathbf{U} - \mathbf{u}) + 2\mathbf{U_n} \cdot \int_0^\infty d^3u \mathbf{u} f_n(\mathbf{r}, \mathbf{u}) \beta_p(\mathbf{r}, \Delta\mathbf{U} - \mathbf{u})$$

$$+ U_n^2 \int_0^\infty d^3u f_n(\mathbf{r}, \mathbf{u}) \beta_p(\mathbf{r}, \Delta\mathbf{U} - \mathbf{u}). \quad (3.3)$$

4. Summary and conclusion

In summary, our major results are (3.1) and (3.2). A tentative comparison of the sources based on the Maxwellian and κ-distribution functions is shown in Fig. 2. It is evident from this figure that the sources based on the Maxwellian distribution function falls off sharply and without any tail region. This therefore excludes the energetic component of the neutral atoms and hence is inappropriate for typical ENAs. By contrast, the sources based on a κ-distribution function depicts a well-behaved tail distribution that represents the ENA distribution.
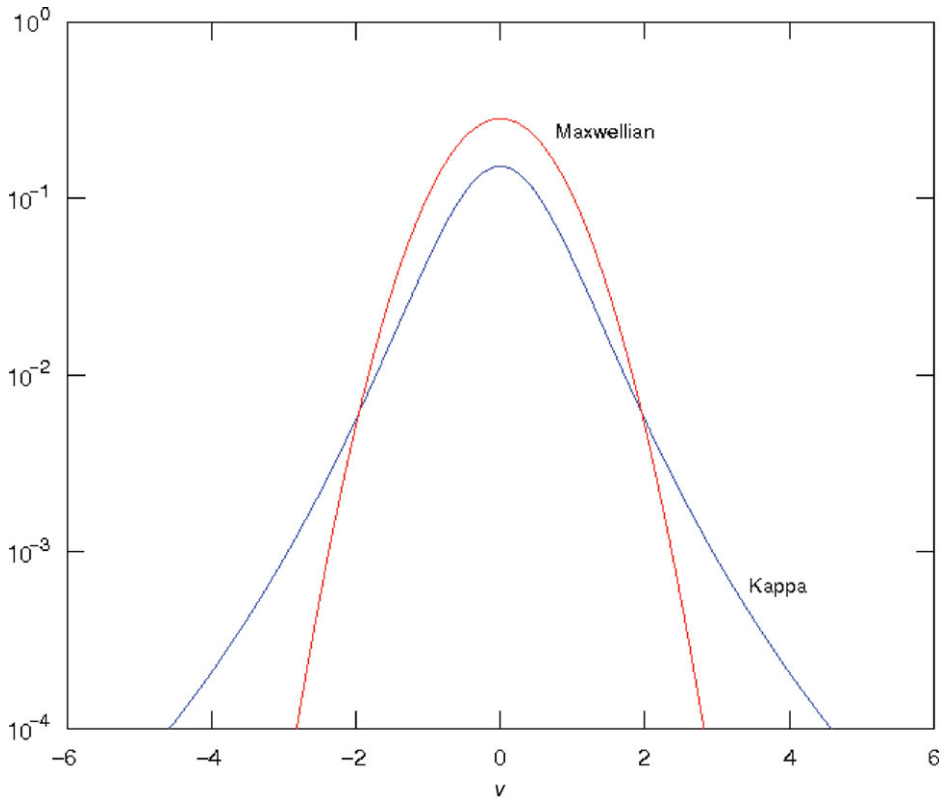
Figure 2. (Colour online) Comparison between the κ- and Maxwellian distribution functions for the sources. Clearly, the tail of the distribution for κ function is long and wide as opposed to the Maxwellian distribution. It is because of this feature, we have computed sources based on the κ-distribution function.

Our previous work in Shaikh and Zank (2008) has shown that charge-exchange modes modify the helioshperic turbulence cascades dramatically by enhancing nonlinear interaction time-scales on large scales. Thus the coupled plasma system evolves differently than the uncoupled system where large-scale turbulent fluctuations are strongly correlated with charge-exchange modes and they efficiently behave as driven (by charge exchange) energy containing modes of helioshperic turbulence. By contrast, small-scale turbulent fluctuations are unaffected by charge-exchange modes, which evolve like the uncoupled system as the latter becomes less important near the larger k part of the helioshperic turbulent spectrum. The neutral fluid under the action of charge exchange tends to enhance the cascade rates by isotropizing the helioshperic plasma turbulence on a relatively long time-scale. This tends to modify the characteristics of helioshperic plasma turbulence, which can be significantly different from the Kolmogorov phenomenology of fully developed turbulence. It remains to be seen how these modified sources influence nonlinear turbulent properties of the small-scale helioshperic plasma fluctuations.

References

Burlaga, L. F., Ness, N. F., Acuna, M. H., Richardson, J. D., Stone, E. and McDonald, F. B. 2009 *Astrophys. J.* **692**, 1125–1130.

Burlaga, L. F. and Ness, N. F. 2009 *Astrophys. J.* **703**, 311.

Burlaga, L. F., Ness, N. F., Acuña, M. H., Lepping, R. P., Connerney, J. E. P. and Richardson, J. D. 2008 *Nature* **454**, 75.

Burlaga, L. F., Ness, N. F. and Acua, M. H. 2006 *Astrophys. J.* **642**, 584.

Decker, R. B., Krimigis, S. M., Roelof, E. C., Hill, M. E., Armstrong, T. P., Gloeckler, G., Hamilton, D. C. and Lanzerotti, L. J. 2005 *Science* **309**, 2020–2024.

Fite, W. L., Smith, A. C. H. and Stebbings, R. F. 1962 *Proc. R. Soc. Lond., Em.* A. **268**, 527.

Goldstein, M. L., Roberts, D. A. and Matthaeus, W. H. 1995 *Ann. Rev. Astron. Astrophys.* **33**, 283.

Heerikhuisen, J., Pogorelov, N. V., Florinski, V., Zank, G. P. and leRoux, J. A. 2008 *Astrophys. J.* **682**, 679.

Heerikhuisen, J., Shaikh, D. and Zank, G. 2007 *AIP Conf. Proc.* **932**, 123.

Mendonca, J. T. and Shukla, P. K. 2007 *Phys. Plasma* **14**(12), 122304–122344.

Pauls, H. L., Zank, G. P. and Williams, L. L. 1995 *J. Geophys. Res.* **A11**, 21595.

Prested, C., Schwadron, N., Passuite, J., Randol, B., Stuart, B., Crew, G., Heerikhuisen, J., Pogorelov, N., Zank, G., Opher, M., et al. 2008 *J. Geophys. Res.* **113**(A6), Cited ID A06102.

Richardson, J. D. 2008 *Plasma Near Termination Shock Heliosheath.* Danvers, MA: AIPC, p. 1039, 418; Li, H., Wang, C. and Richardson, J. D. 2008 *Geophys. Res. Lett.* 3519107.

Shaikh, D. and Zank, G. P. 2010 *AIP Conf. Proc.* **1216**, 164–167.

Shaikh, D. In press *J. Plasma Phys.*, 2009arXiv0912.1568S.

Shaikh, D., Zank, G. P. and Pogorelov, N. 2006 *AIP Conf. Proc.* **858**, 308–313.

Shaikh, D. and Zank, G. P. 2008 *Astrophys. J.* **688**(1), 683–694.

Shukla, P. K. 1978 *Nature* **274**, 874.

Stone, E. C., Cummings, A. C., McDonald, F. B., Heikkila, B. C., Lal, N. and Webber, W. R. 2005 *Science* **309**, 2017–2020.

Zank, G. P. 1999 *Space Sci. Rev.* **89**, 413–688.